Intense source of cold Rb atoms from a pure two-dimensional magneto-optical trap

J. Schoser, A. Batär, R. Löw, V. Schweikhard, A. Grabowski, Yu. B. Ovchinnikov, and T. Pfau
5. Physikalisches Institut, Universität Stuttgart, Pfaffenwaldring 57, 70550 Stuttgart, Germany
(Received 16 January 2002; published 26 August 2002)

We present a two-dimensional (2D) magneto-optical trap (MOT) setup for the production of a continuous collimated beam of cold ^{87}Rb atoms out of a vapor cell. The underlying physics is purely two-dimensional cooling and trapping, which allows for a high flux of up to 6×10^{10} atoms/s and a small divergence of the resulting beam. We analyze the velocity distribution of the 2D MOT. The longitudinal velocity distribution of the atomic beam shows a broad feature (full width at half maximum $\simeq 75$ m/s), centered around 50 m/s. The dependence of the flux on laser intensity, on geometry of the trapping volume, and on pressure in the vapor cell was investigated in detail. The influence of the geometry of the 2D MOT on the mean velocity of the cold beam has been studied. We present a simple model for the velocity distribution of the flux based on rate equations describing the general features of our source.

DOI: 10.1103/PhysRevA.66.023410 PACS number(s): 32.80.Pj, 07.77.Gx, 03.75.Be

I. INTRODUCTION

Cold atomic beams are needed for many applications in atom optics [1,2] or in the field of atomic clocks based on atomic fountains. In particular, the process of evaporative cooling [3] demands a high atom number as a starting point to reach quantum degeneracy. This requires an intense source which can efficiently load a magneto-optical trap (MOT) in UHV fast.

For this purpose sources with a small divergence of the atomic beam are favorable. The longitudinal velocities in the beam should be within the capture range of the three dimensional (3D) MOT. As long as the cross section of the beam is smaller than the spatial capture range of the MOT the figure of merit for optimized loading into a MOT is the total integrated flux up to its capture velocity.

Sources that are common in many experiments are cooled atomic beams in the form of either a chirped slower [4] or a Zeeman slower [5]. A Zeeman slower decelerates an intense thermal atomic beam along the propagation axis of the beam by radiation pressure, while the spontaneous emission processes give rise to a transverse heating of the atoms. This emerges in a strongly diverging beam with a flux of up to 10^{11} atoms/s. The divergence might impose geometrical constraints on the arrangement of the Zeeman slower's output and the trapping volume of the 3D MOT. In some cases the slowing light on axis or the magnetic fields involved disturb the following MOT.

In comparison MOT sources provide advantages like a compact setup, smaller magnets are used, they provide a well collimated beam of cold atoms, and have a reduced background of thermal atoms. Let us first discuss pulsed 3D MOT sources. Atoms are collected from a vapor into a 3D MOT and then extracted from it. There are different ways to extract the atoms: by letting the atoms fall in gravity [6], by a pushing beam [7], or simply by an imbalance in radiation pressure [8]; also in combination with a magnetic confinement along the transfer tube [9], by release into a moving molasses [10], and by moving magnetic fields [11]. In this pulsed regime an integrated flux of several 10^9 atoms/s was achieved.

Another step in the evolution of cold atom sources are continuous 3D MOT sources. The first significant breakthrough for this source type was realized by Lu *et al.* who developed a low velocity intense source (LVIS) of atoms by creation of a dark channel in one of the six MOT laser beams [12]. It reaches a flux of 5×10^9 atoms/s. Generally, a 3D MOT with a hole in one of the laser beams creates a narrow beam of cold atoms [13,14]. Due to the imbalance in the radiation pressure along one axis a continuous beam of cold atoms is coupled out of a trapped cloud. This source provides a small thermal background and a narrow velocity profile at velocities below 20 m/s.

Another approach is two-dimensional magneto-optical cooling. This technique was first used to cool and compress transversally atomic beams [15–19]. It has been demonstrated that two-dimensional cooling, applied in different configurations, produces a beam of cold atoms out of a vapor cell [20–22]. Dieckmann *et al.* [21] realized a 2D MOT including axial beams which produces a total flux of 9×10^9 ^{87}Rb atoms/s. This setup uses small cooling laser powers and retroreflection of the laser beams.

Pure 2D cooling does not require light on the axis of the atomic beam compared to a Zeeman slower, a LVIS, or a 2D MOT as in [21]. Hence there is less disturbance of the following 3D MOT setup. Radial cooling collimates the outgoing beam while the allowed cooling time, which depends on the geometry of the cooling region, influences the possible longitudinal velocities of atoms in the beam. The resulting flux is comparable to that of a Zeeman slower. Moreover it offers a small beam divergence.

The purpose of this paper is to study the total flux of a 2D MOT setup at elevated vapor pressures and without retroreflecting the cooling laser beams; to study the dependence of the flux on length, laser power, and pressure in the vapor cell; and to develop a theoretical model for the description of the main features of the source.

This paper is organized as follows. In Sec. II we explain the basic principle of a two-dimensional MOT. We discuss the influence of geometry, laser power, and pressure in the vapor cell on the atomic beam. Based on rate equations we derive a model for the longitudinal velocity distribution. In Sec. III we present a detailed description of the setup and the

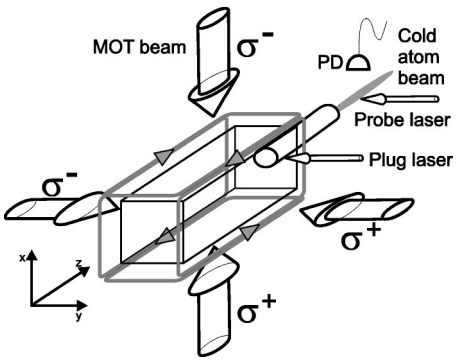

FIG. 1. Schematic view of the setup. Rectangular coils produce a two-dimensional magnetic quadrupole field. The line of zero magnetic field coincides with the long axis of the glass cell. Four perpendicular laser beams with circular polarizations in the usual MOT configuration cool the atoms in two dimensions. The atomic beam travels horizontally through a differential pumping tube. Analysis of the beam is done by a time-of-flight-method. A plug beam shuts off the atomic beam and a probe laser is shone in perpendicularly to the beam. The fluorescence is detected by a calibrated photodetector.

measurement techniques used for the characterization of the cold atomic beam. The experimental results are presented in Sec. IV. We summarize and give an outlook on future steps in our experiment in Sec. V.

II. PRINCIPLE OF OPERATION AND THEORETICAL MODEL

A. Principle of operation

The basic principle of a 2D MOT is laser cooling of an atomic vapor in two dimensions. The interplay of a finite cooling time and a geometrical filter allows one to extract only slow atoms from a vapor cell.

Two orthogonal pairs of counterpropagating laser beams are shone into a vapor cell. In combination with a two-dimensional magnetic quadrupole field the light creates a radial restoring force toward the line of zero magnetic field and thus enclose a finite cooling volume. The geometry is shown in Fig. 1 and a more detailed description is given in Sec. III. Atoms from the vapor which enter the cooling volume are slowed down in the two radial dimensions and are compressed onto the z axis. The velocity of the atoms in the longitudinal direction is not changed. Hence the atoms travel on a skewed trajectory into the center of the 2D MOT, while propagating along the axis. This produces two antiparallel, thin, dense, and well collimated atomic beams. We restrict our treatment to one beam traveling in the positive z direction, where it passes through a differential pumping tube into a UHV chamber.

The atoms in the vapor cell have to satisfy three criteria simultaneously in order to contribute to the flux of laser-cooled slow atoms at the exit of the differential pumping tube.

(a) The radial component of the initial velocity needs to be smaller than the transverse capture velocity of the 2D MOT.

(b) The interaction time of the atoms with the light field needs to be long enough so that the trajectory of the atom hits the entrance of the differential pumping tube (the radial velocity is sufficiently cooled) such that its divergence is small enough to reach the exit of the tube.

(c) The mean free path in the vapor cell should be larger than or comparable to the trajectory of the atoms, so that they are not removed from the atom beam due to collisions.

B. Assumptions for the theoretical model

For the following theoretical model we assume that the 2D MOT is loaded from a thermal atomic vapor obeying a Maxwell-Boltzmann distribution. The cooling volume is approximated as a cooling cylinder which is oriented along the z axis. We neglect the Gaussian beam profile and suppose a uniform distribution of laser light within the volume of the cooling cylinder. The absorption of the cooling laser beams in the vapor cell is also neglected. The heating of atoms due to spontaneous emission and reabsorption is not considered since it does not produce a large change in the longitudinal velocity. Collisions can take place only in the vapor cell. After the atoms leave the cooling cylinder they undergo no further collisions in the differential pumping tube.

C. Influence of geometry

Let us first consider the collisionless regime where the density is low enough that the mean free path in the vapor cell is larger than the dimensions of the cell. In this case we can assume that the thermal atoms start on the walls and no collisions take place in the volume. The geometry of the tube and the glass cell is designed in such a way that the opening angle of the differential pumping tube does not accept atoms starting on the sidewalls without being transversely cooled. In this configuration thermal atoms are only transmitted if they start on that part of the back wall of the glass cell which lies within the acceptance angle of the differential pumping tube. Its choice limits the thermal background. For an understanding of the total flux and its dependence on the geometry, the longitudinal velocity profile of the atomic beam needs to be investigated.

The concept of a capture velocity, well known from 3D magneto-optical traps, must be modified to embrace the 2D MOT configuration. Since the cooling is restricted to transverse velocities, we define a radial capture velocity. In spherical 3D MOTs the capture velocity depends on detuning, on laser beam size and intensity, and on the magnetic field gradient. However, in a 2D MOT a finite cooling time is necessary to collimate the atoms onto the beam axis. Atoms which travel too fast along the z direction cannot be sufficiently cooled and are filtered out by the aperture. A main parameter is therefore the cooling time $\tau = z/v_z$ which is given by the longitudinal velocity v_z and the distance z from the tube at which the atom enters the cooling volume of the 2D MOT. Thus the effective transverse capture velocity becomes a function of z and v_z. For small v_z the radial cooling time dominates and the capture velocity should be simply a constant v_{c0} determined by the parameters of the cooling laser beams and the magnetic field gradient. For larger v_z the

capture velocity should fall off as $1/v_z$. The velocity range between these two asymptotes depends additionally on the position z where atoms enter the cooling volume. With increasing cooling length one should expect more atoms with high axial velocities to be transversely cooled and transmitted through the tube.

The cooling time τ determines the final transverse velocity: $v_{r,i}-v_{r,f}=(1/m)\int_0^\tau F_{sp}(x(t),v(t))dt$. Here F_{sp} is the spontaneous scattering force, $v_{r,i}$ the initial and $v_{r,f}$ the final radial velocity, and m the mass of a Rb atom. By that the divergence of the atomic beam (if it is not limited by the acceptance angle of the tube) is shaped depending on the mean length of the cooling volume. Radial cooling within a finite cooling time increases the portion of atoms with small v_z in the beam. *This is the reason why the velocity distribution of the atomic beam is nonthermal and is shifted to much lower values than a thermal distribution* at room temperature ($\langle v\rangle \simeq 275$ m/s) although there is no longitudinal cooling. A typical time scale for the cooling time is 1–2 ms. As described in Sec. III, the usual length of the cooling volume in our setup is about 60 mm. This gives a rough estimate for the mean velocity in the atomic beam between 30 and 60 m/s.

The transverse beam size, in combination with detuning and magnetic field gradient, determines the radial capture velocity v_{c0}. An increase of the longitudinal beam size (along the z axis) increases the upper limit of the longitudinal velocities that are trappable. Additionally, the size controls the mean longitudinal velocity in the beam of cold atoms, which increases with increasing MOT length. Hence the total flux should grow with the length of the 2D MOT. In the limit of an infinitely long 2D MOT the longitudinal velocity distribution of the atom beam becomes equal to a thermal distribution.

The influence of the MOT laser intensity is reflected in the efficiency of the transverse cooling. The capture velocity should increase with intensity and saturate at some value when the saturation parameter dominates the spontaneous force.

Without collisions the number of trappable atoms and thereby the flux increases with pressure in the vapor cell.

D. Influence of collisions

Let us now discuss the effect of collisions. At higher pressures collisions lead to a thermalization of the atoms in the volume of the vapor cell. Thereby atoms can now start not only from the walls but also from within the vapor cell. This increases the background of thermal atoms in the atomic beam. Moreover, background gas collisions in the vapor cell and light assisted collisions of excited atoms in the beam with the background gas are mechanisms that limit the flux when the MOT length increases. The mean number of collisions is given by the product of an ensemble averaged collision rate $\Gamma=n\sigma\langle v\rangle$ and the mean time $\tau=\langle z\rangle/v_z$ which the atom spends in the cooling volume. n is the density in the vapor cell, σ the collision cross section, and $\langle v\rangle$ the mean thermal velocity in the vapor cell. The longer the MOT is, the longer becomes the time of propagation that the atoms spend in the vapor cell. Therefore the higher is the probability for losses due to collisions such that a further increase of MOT length does not produce a higher flux. In this simple picture the flux is supposed to saturate as a function of MOT length. The mean velocity should increase since atoms with small v_z are more affected by collisions.

For a given MOT geometry an increasing pressure will decrease the effective length of the cooling volume. Therefore one should expect an optimum pressure for a given geometry of the 2D MOT, namely, when the mean free path in the vapor cell becomes comparable with the length of the cooling volume. In addition higher densities in the vapor cell lead to absorption of the laser beams, which decreases the cooling efficiency.

E. Rate equation model

For a theoretical description of the flux of cold atoms from a 2D MOT source we resort to a simple rate model which was introduced in [23] for vapor-cell MOTs and later expanded for atomic beam sources in [21]. Based on that model for the total flux we derive a model for the longitudinal velocity distribution of the atom flux.

We define a function $\hat{\Phi}$ which describes the integrated flux per velocity interval $[v_z, v_z+dv_z]$:

$$\hat{\Phi}(n,v_z)=\frac{\int_0^L R(n,v_z,z)\exp(-\Gamma_{coll}(n_{tot})z/v_z)dz}{1+\Gamma_{trap}(n_{tot})/\Gamma_{out}}. \quad (1)$$

Here Γ_{trap} is the loss rate out of the trapped cloud due to background gas collisions, Γ_{out} determines the outcoupling rate from the captured vapor in the 2D MOT trapping region into the atomic beam. L is the total length of the cooling volume, n_{tot} is the total density of all Rb isotopes, and n is the density of ^{87}Rb atoms in the vapor cell ($n=0.28n_{tot}$). R is the loading rate of ^{87}Rb atoms into the 2D MOT. The effect of light assisted collisions between the background gas and the cold atoms in the atomic beam on the way to the tube (described by the collision rate Γ_{coll}) is implemented by an exponential loss term. In our setup the cooling region extends directly to the differential pumping tube. z/v_z is the time of flight for the atoms through the MOT volume.

The total flux, which gives the number of atoms per time interval integrated over the output area of the source, is given by the integral of $\hat{\Phi}$ over all longitudinal velocities: $\Phi=\int_0^\infty \hat{\Phi}(n,v_z)dv_z$. Only positive values for v_z are taken into account.

In order to derive the loading rate for a 2D MOT, one needs to consider the flux of atoms through the surface of the cooling volume. Since we are interested in the loading flux through the sidewalls, we need to consider only radial velocities, weighted with that part of the Boltzmann distribution which is trappable according to the discussion above. The loading rate is proportional to the density in the vapor cell and to the surface area of the cooling volume. We define a loading rate per velocity interval $[v_z, v_z+dv_z]$:

$$R(n,v_z,z)=nd\frac{16\sqrt{\pi}}{u^3}\exp\left(\frac{-v_z^2}{u^2}\right)\times\int_0^{v_c(v_z,z)}v_r^2\exp\left(\frac{-v_r^2}{u^2}\right)dv_r, \quad (2)$$

where d is the diameter of the cooling volume, $u=\sqrt{2k_BT/m}$ is the most probable velocity of the Maxwell-Boltzmann distribution with k_B denoting the Boltzmann constant and T the temperature of the vapor, and $v_r=\sqrt{v_x^2+v_y^2}$ is the radial velocity. The integral's upper limit v_c is the capture velocity which is generally a function of the longitudinal velocity v_z and of the atom's distance z from the aperture.

To satisfy the two asymptotic behaviors at low v_z ($v_c\rightarrow v_{c0}=\text{const}$) and at high v_z ($v_c\propto 1/v_z$) we model v_c as

$$v_c(v_z,z)=\frac{v_{c0}}{1+v_z/v_{cr}}. \quad (3)$$

v_{c0} is the radial capture velocity which lies usually in the range of 30 m/s. v_{cr} is the so-called critical velocity above which the cooling time is limited by the longitudinal motion and the capture velocity falls off as $1/v_z$. The capture velocity is nearly equal to v_{c0} below v_{cr}. We choose v_{cr} via the equality of the mean longitudinal flight time $L/(2\,v_{cr})$ and the radial cooling time which we approximate by d/v_{c0}. In this approximation the explicit z dependence of v_c drops out. This results in $v_{cr}=Lv_{c0}/(2d)$.

This gives for the flux per velocity interval

$$\hat{\Phi}(n,v_z)=\frac{nd}{1+\Gamma_{trap}(n_{tot})/\Gamma_{out}}\frac{16\sqrt{\pi}}{u^3}\frac{v_z}{\Gamma_{coll}(n_{tot})}\times\exp\left(\frac{-v_z^2}{u^2}\right)\left[1-\exp\left(-\Gamma_{coll}(n_{tot})\frac{L}{v_z}\right)\right]\times\int_0^{v_c}v_r^2\exp\left(\frac{-v_r^2}{u^2}\right). \quad (4)$$

At residual vapor pressures of a few 10^{-7} mbar the typical lifetime of a MOT loaded from atomic beams is about 100 ms. From that we conclude a collision rate Γ_{trap} on the order of 10 s^{-1} for this vapor pressure. As will be discussed in Sec. IV the typical cooling time is in the range of milliseconds; therefore the order of magnitude for Γ_{out} is 10^3 s^{-1}. The collision rate for light assisted collisions is given by $\Gamma_{coll}=n_{tot}\langle v\rangle\sigma$, where $\langle v\rangle$ is the mean velocity in the vapor, and σ is the effective collision cross section for light assisted collisions between the background gas atoms and atoms in the cold beam. Following [21,24] we assume that this process can be described by the resonant dipole-dipole interaction and follows a C_3/R^3 potential. R is the interatomic distance.

When fitting the experimental results with this theoretical model we obtain $\Gamma_{trap}/\Gamma_{out}=0.012$ at a pressure of 10^{-7} mbar. This agrees well with the observed lifetimes. For the effective collision cross section we get $\sigma_{eff}\approx 1.8\times 10^{-12}$ cm^2. This value matches within a factor of 2 with the measurement of Dieckmann *et al.* [21].

When comparing the theoretical results with the experiment, Eq. (4) needs to be multiplied by an overall scaling factor. The fit to our measured data yields a scaling factor of 2×10^{-2}. This might be attributed to the absorption of the cooling laser in the Rb vapor or to a deviation of our pressure estimation from the real value. Eq. (4) describes the longitudinal velocity distribution in the cold atomic beam. A comparison of this model with the measured results will be given in Sec. IV.

F. Summary

Let us summarize the expected general behavior.

(1) An increasing MOT length should lead to the following.

(*a*) *A higher flux*. Faster atoms can be captured with increasing L. Due to collisions the expression of $\hat{\Phi}(n,v_z)$ becomes independent of L for large values of L. The flux shows a saturation for lengths above $L>\langle v_z\rangle/\Gamma_{coll}(n)$.

(*b*) *An increasing mean velocity in the atomic beam*. Above an optimum MOT length every increase in length will only add faster atoms to the beam, thus increasing the value for the mean velocity.

(2) An increasing density of Rb atoms in the vapor cell should lead to the following.

(*a*) *A linear increase of the total flux at low pressures*. The loading rate is proportional to $n/[1+\Gamma_{trap}(n)/\Gamma_{out}]$ which is linear in the density for low pressures. At higher pressures the term $1/\Gamma_{coll}(n)$, which is inversely proportional to n, dominates. For a given length of the MOT beams there exists an optimum pressure above which the flux decreases with increasing pressure.

(*b*) *An increasing mean velocity*. The necessary momentum transfer to be pushed out of the beam is smaller for slow atoms, leaving a higher fraction of faster atoms in the beam.

III. EXPERIMENTAL SETUP AND DIAGNOSTICS

The basic geometry of the experimental setup (see Fig. 1) is given by a vapor cell separated from a UHV chamber by a differential pumping tube which is also the aperture for the output beam of cold atoms. The tube is conically shaped, 133 mm long, and has a diameter of 6 mm which widens at the UHV end up to 9.6 mm. It maintains a pressure drop of three orders of magnitude between a vapor pressure cell and two UHV six-way crosses used as analyzing chambers. Compared to other setups we use a rather large aperture for the differential pumping tube. We have implemented a shutter inside the differential pumping tube on the side of the vapor cell which can be operated by a rotary motion feedthrough. Hence the UHV cannot be excessively loaded by thermal atoms. The vapor cell is a glass cuvette (135 mm$\times$35 mm$\times$35 mm) whose long axis (z axis) is horizontally aligned.

Electric heating rods around the glass cell provide homogeneous and stable heating thus allowing one to work at relatively high vapor pressures between 10^{-7} and

3×10^{-6} mbar. Four rectangularly shaped, elongated magnetic coils are placed around the vapor-cell producing a two-dimensional quadrupole field. The axes of both the cell and the tube coincide with the line of zero magnetic field (z axis) which is horizontal. We work with a field gradient of 17 G/cm.

Cooling laser light is provided by a Ti:sapphire laser. The laser is red detuned by 1.9Γ ($\Gamma=2\pi$ 6 MHz) from the $5S_{1/2}$, $F=2\rightarrow5P_{3/2}$, $F=3$ transition. To repump atoms back into the cycling transition an external cavity diode laser is employed that is stabilized to the $5S_{1/2}$, $F=1\rightarrow5P_{3/2}$, $F=2$ transition. For the analysis of the atomic beam another diode laser is used. This probe laser is locked on resonance to the $5S_{1/2}$, $F=2\rightarrow5P_{3/2}$, $F=3$ transition.

The light of the cooling laser is split into four separate beams which are expanded in spherical and cylindrical telescopes placed in sequence up to a beam size of roughly 95×15 mm^2 (horizontal waist radius $w_z\approx25$ mm, vertical waist radius $w_\rho\approx6$ mm). Two pairs of horizontally and vertically counterpropagating beams with orthogonal circular polarizations in the usual MOT configuration are overlapped in the center of the glass cell. Thus they enclose a cooling volume along the axis of zero magnetic field. The repumping light is overlapped with two horizontal beams. In order to work at high vapor pressures it is necessary to use four different laser beams. Retroreflection of the light beams would lead to a strong imbalance in the light pressure due to the high absorption in the vapor.

The center of the 2D MOT laser beams is positioned about 40 mm in front of the entrance edge of the differential pumping tube. The cooling volume extends to the front of the tube. There is no dark distance which the atoms travel at background pressure without being transversely cooled. This upholds the good collimation of the beam until it leaves the vapor cell.

Diagnostics

The measurement of the Rb pressure in the cell is accomplished by absorption measurement. The frequency of a small laser beam whose intensity is below saturation is swept across resonance. The measurement is calibrated by the absorption of Rb vapor at room temperature whose vapor pressure is 10^{-7} mbar [26].

Information about the transverse capture velocity of the 2D MOT can be obtained by Doppler spectroscopy perpendicular to the atomic beam in the vapor cell. For that purpose a probe laser beam with a diameter of 1 mm is aligned through the atomic beam orthogonally to its axis onto a photodiode. When its frequency is swept across resonance the Doppler profile reveals a Gaussian shape due to the thermal velocity distribution of the atoms with two dips symmetrically centered around the maximum. Atoms of the velocity classes corresponding to the dips have been cooled and therefore the height of the central part corresponding to the cold atoms increases. Division by the fitted Gaussian profile shows this structure clearly (Fig. 2). Half of the width between the minima corresponds to the capture velocity.

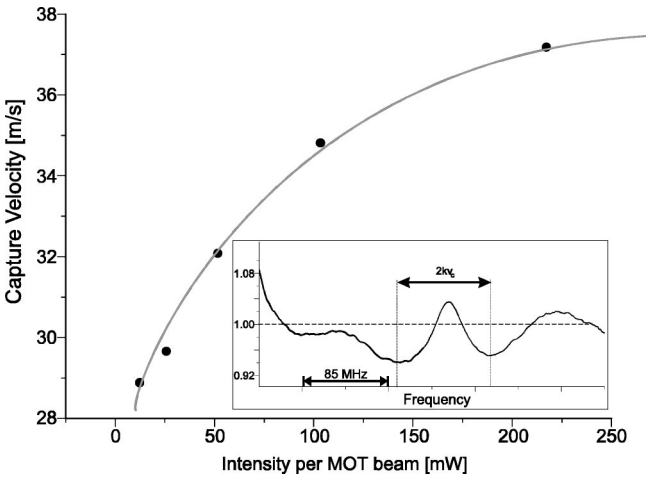

FIG. 2. Transverse capture velocity of the 2D MOT. The inset shows the normalized Doppler spectroscopy signal, i.e., the measured signal divided by a fitted Gaussian distribution. The width between the two minima corresponds to twice the capture velocity. The main graph shows the dependence of the capture velocity on the intensity in the cooling laser beams. The line serves merely to guide the eye. The capture velocity saturates at high intensities at a value of 38 m/s. This is about the linear capture range which is obtained when equating the frequency shift due to the Zeeman effect with the detuning of the laser.

The transverse beam profile is investigated in the UHV part of the setup. A probe beam with a diameter of 1 mm is directed orthogonal on the atomic beam. Perpendicular to it a charge-coupled device camera images the fluorescence signal. From the increasing full width at half maximum of the signal when moving the probe beam along the z axis the divergence of the atomic beam is quantified.

The analysis of the longitudinal velocity distribution of the atomic beam is done by a time-of-flight (TOF) method. A fraction of the MOT laser intensity is split off and shone into the vapor cell directly in front of the tube perpendicular to the atomic beam axis. This beam has a diameter of ≈8 mm, and its power was held constant at 150 mW throughout all measurements. It deflects all atoms with a longitudinal velocity lower than 130 m/s and hence plugs the atomic beam for all smaller velocities. After a flight distance of 145 mm a light sheet of 1 mm width from a probe laser is used to irradiate the atomic beam in the UHV chamber orthogonal to the atom beam. A fraction of the repumping light is overlapped with the probe laser. A calibrated photodiode detects the fluorescence of the atoms. After plugging the atomic beam the fluorescence signal fades out. From this signal information about the velocity distribution of the atomic flux can be derived according to

$$\Phi(v_z)=\frac{\eta}{d_{probe}}\frac{l}{v_z}\frac{dS}{dt}, \tag{5}$$

where S is the fluorescence signal from the photodiode, d_{probe} is the width of the probe beam light sheet, l is the distance between plug beam and probe beam, and η contains calibration parameters of the detection system.

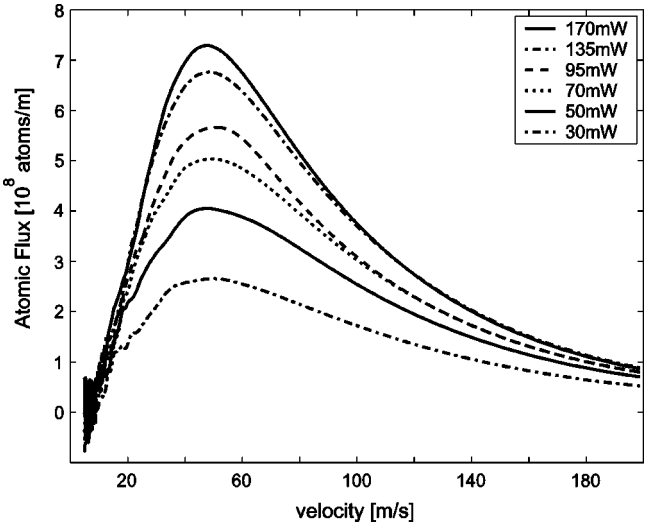

FIG. 3. Distribution of the atomic flux versus the longitudinal velocity. The laser power in the cooling beams was varied from 30 mW to 170 mW. The pressure for this measurement is 1.6×10^{-6} mbar; the length is 92 mm. A small shift of the mean velocity to higher values with increasing laser power is visible. The velocity distribution is centered around 50 m/s and has a width of about 75 m/s.

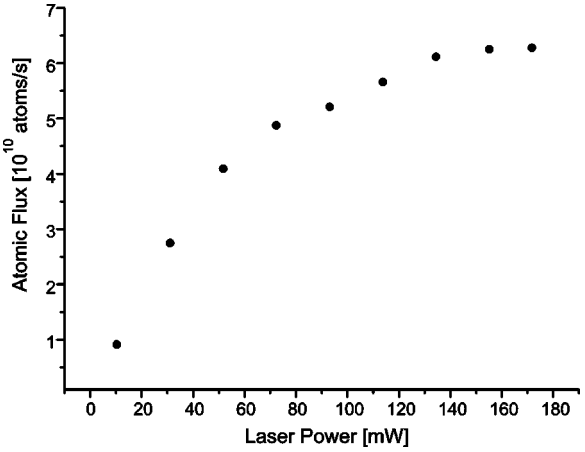

FIG. 4. Dependence of the total atomic flux on the cooling laser power per beam. The total flux in atoms/s is given by the area under the curves in Fig. 3. It ranges from 1×10^{10} to 6×10^{10} atoms/s. The total flux depends strongly on laser power and saturates at values of 160 mW per laser beam.

IV. EXPERIMENTAL RESULTS

First we give information about the characteristics of the 2D MOT: its loading time and its capture velocity. This is followed by a discussion of the properties of the atomic beam. The influence of laser power, length of the cooling volume, and the pressure in the vapor cell is studied.

A. Characteristics of the 2D MOT

The two-dimensional laser cooling produces a line about 2 mm wide and 90 mm long of high intensity fluorescence light in the glass cell along the axis of zero magnetic field, which is clearly visible at low vapor pressures.

A measurement of the radial capture velocity in the way described above yields the maximum transverse capture velocity v_{c0} in Eq. (3). The capture velocity depends on the intensity of the laser beams, the detuning, and the magnetic field gradient. Figure 2 displays the dependence of v_{c0} on the laser intensity. The inset shows the Doppler spectroscopy signal from which the capture velocity is inferred. In the intensity range which we apply, it extends from 28 m/s to 38 m/s. For high laser powers above 160 mW per beam (which corresponds to an average intensity of $\simeq 17$ mW/cm^2 per beam) it saturates at a value of 38 m/s. This value matches well with an estimate from equating the frequency shift due to the Zeeman effect with the detuning of the laser, which gives the linear capture range—in our case 35 m/s.

For measuring the loading time of the 2D MOT we directed a 1 mm thick probe laser beam through the center of the atomic beam onto a photodiode. When the 2D MOT cooling light was switched on the absorption decreased abruptly because the $F=2\rightarrow F=3$ transition is driven by the MOT laser. The absorption increases again and reaches a steady state when the atoms are transversely cooled and closer in resonance with the probe laser than with the MOT light. The $1/e$ time of this increase is about 2 ms. This gives the characteristic time scale for the cooling process. From that we estimate the value for the outcoupling rate Γ_{out} in Eq. (4) to be on the order of 10^3 s^{-1}.

The emerging atomic beam is well collimated. From our transverse beam profile measurement we deduce a beam divergence of 32 mrad. This is about a factor of 2 less than the divergence geometrically allowed by the differential pumping tube of 59 mrad. This means that the beam of cold atoms is not hindered by the aperture. It is possible to further suppress the thermal background by diminishing the aperture of the differential pumping tube without decreasing the flux of cold atoms in future experiments.

B. Velocity distribution

The time-of-flight measurements give information about the distribution of the atomic flux versus velocity. A typical set of velocity distributions is depicted in Fig. 3. The varied parameter for the single curves is the power in the laser beams. We observe a relatively broad feature with a peak velocity of around 50 m/s and a width of roughly 75 m/s. An increase of the peak velocity with increasing laser power is visible. The transverse cooling works more efficiently with increasing laser intensity. Therefore atoms with a higher velocity in the z direction contribute to the beam. The integral of the flux distribution gives the total flux of atoms per unit time. This is displayed in Fig. 4. The total flux saturates for laser powers above 160 mW per laser beam. We observe a maximum flux of 6×10^{10} atoms/s at a laser power of 160 mW per laser beam and at a vapor pressure of 1.8×10^{-6} mbar.

C. Length dependence

In addition to the field gradient and the detuning, the size of the MOT beams determines the capture range of the MOT.

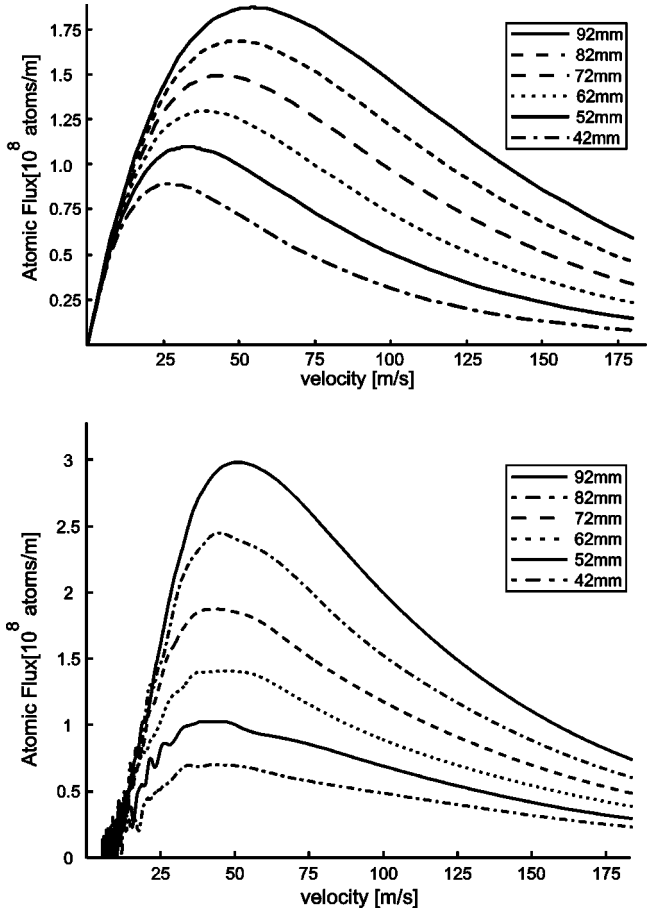

FIG. 5. Dependence of the atomic flux on the length of the MOT beams. The upper graph shows the prediction by our model. The experimental result is plotted in the lower graph. The power per laser beam is held constant at 21 mW and the Rb pressure is 1.6×10^{-6} mbar. The peak of the velocity distribution is shifted to higher values for a longer cooling volume. The atomic flux increases with the length of the cooling volume. In this measurement an increasing part of the MOT beams is blocked while the laser power is adjusted so that the total laser power incident on the atoms stays constant.

As discussed in Sec. II the length of the cylindrical MOT beams strongly influences the flux of cold atoms. Figure 5 shows the distribution of the atomic flux versus velocity when the length of the beams is varied. The upper part shows the result of our theoretical model. The lower part displays the TOF results. This measurement was done by successively blocking a part of all four cylindrical MOT beams starting on the back side of the glass cell. The laser power per beam for the full-length 2D MOT was 50 mW. Therefore the total flux for the maximum length is about 3.5×10^{10} atoms/s. While decreasing the length of the 2D MOT we simultaneously increased the laser power per beam so that the power shining on the atoms was kept constant. Thus it is ensured that we see the pure influence of the MOT length at a given constant available laser power. With increasing length the flux grows and the maximum velocity shifts to higher values, which agrees with our predictions in Sec. II. Figure 6 shows the total flux as a function of the MOT length. The total flux is

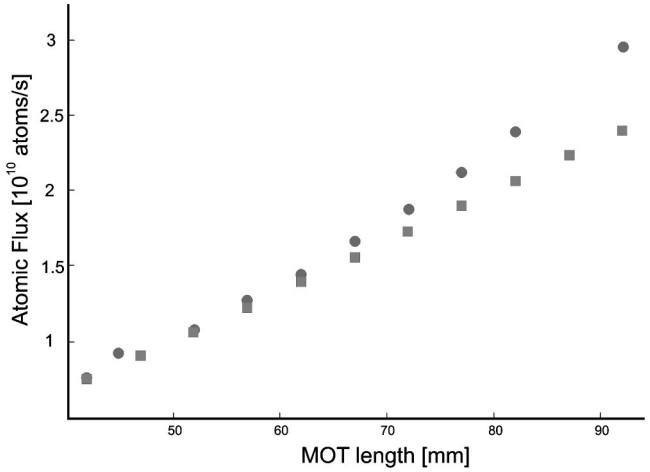

FIG. 6. Dependence of the total flux on the length of the cooling volume. The experimental parameters are the same as in Fig. 5. The squares show the theoretical and the circles the experimental data.

expected to saturate for a cooling volume above an optimum length which is given by the mean velocity and the collision rate $\Gamma_{coll}(n)$ as discussed in Sec. II. However, for the pressure range of this measurement no saturation of the flux is visible even at the maximum MOT length of 92 mm. Confirming the discussion in Sec. II, we observe that the maximum velocity shifts toward higher values when the MOT length increases. Our model is in good agreement with the measurements and predicts the essential features that we observe. Only the width of the velocity distribution is not accurately described.

D. Pressure dependence

The variation of the Rb vapor pressure is done by changing the temperature of the glass cell in a controlled way. It is possible to raise the vapor pressure from 1×10^{-7} mbar to 3×10^{-6} mbar. Figure 7 demonstrates the dependence of the velocity distribution on the vapor pressure. The upper part shows the behavior as described by our theoretical model; the lower graph displays the TOF measurements. The flux increases with increasing pressure, reaches a maximum at 1.5×10^{-6} mbar, and decreases again for higher pressures. In the high pressure regime the mean free path of Rb atoms in the vapor cell is of the order of a few centimeters and is comparable to the dimensions of the atomic beam in the 2D MOT. This means that collisions start to limit the atomic flux as is discussed in Sec. II. Above the optimum pressure value the total flux decreases again. The optimum pressure depends on the length of the 2D MOT. The longer the 2D MOT, the smaller is the value for the optimum pressure. Our value for the optimum pressure agrees well with the prediction of Vredenbregt *et al.* [25].

The maximum velocity of the distribution shifts toward higher values with increasing pressures. This is revealed in the experiment and also in the theoretical curves. Atoms with a small longitudinal velocity are more affected by collisions because a small transverse momentum transfer already produces a large enough divergence so that the atoms collide

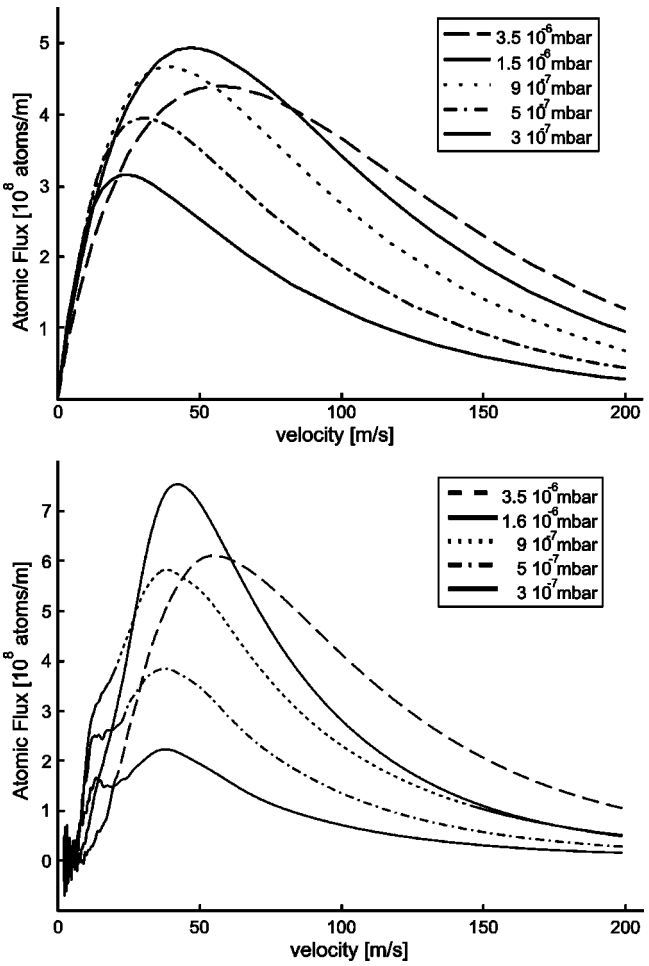

FIG. 7. Distribution of the atomic flux versus the longitudinal velocity. The pressure in the vapor cell was varied from 10^{-7} mbar to 3.5×10^{-6} mbar. The upper graph shows the results of our model. The experimental results are plotted in the lower graph. The model describes an increase in the peak velocity with increasing pressure and also a growing flux with higher pressures, which is in accordance with the experimental results. Above an optimum pressure the flux decreases again. This is also visible in the dashed line both in the model and in the measurement.

with the tube. A higher pressure leads to a larger mean velocity in the atomic beam.

The total flux as a function of vapor pressure is shown in Fig. 8. The linear increase of the flux at low pressures and the existence of an optimum pressure are well described by our model.

We verified the results of the TOF technique with the method of Doppler spectroscopy directly on the atomic beam. For that purpose another light sheet from the probe laser was aligned counterpropagating to the atomic beam at an angle of 3.5° to it. When scanning the laser frequency one obtains Doppler profiles that confirm the longitudinal velocity profiles of the beam obtained by the TOF measurements. In this measurement we could verify that the integrated flux of thermal atoms transmitted by the differential pumping tube is only about 10% of the flux of cold atoms.

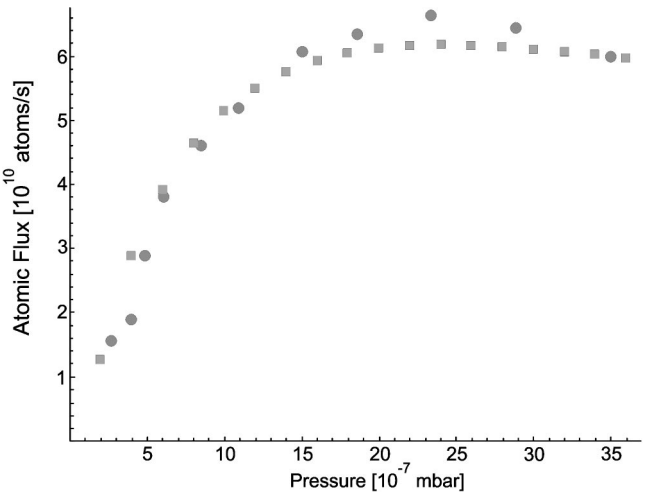

FIG. 8. Dependence of the atomic flux on the Rb pressure in the vapor cell. The squares mark the theoretical results whereas the circles describe the experimental results. The measurement was done at full length of the MOT laser beams (92 mm) and at a laser power of 170 mW. At low pressures the atomic flux increases linearly whereas it finds a maximum at about 2×10^{-6} mbar and decreases for higher values. The mean free path in the cell reaches the value of the length of the MOT at the pressure for the maximum flux—a clear hint that collisions limit further increase of the atomic flux. The theoretical model agrees well with the experimental data.

E. Pushing beam

In addition to the Doppler-cooling laser light we shone in a laser beam of the same detuning with a diameter of 5 mm on the axis copropagating with the atoms (pushing beam). The longitudinal velocity distribution in this case is shown in Fig. 9. A narrow (width $\approx$7.5 m/s) and intense peak at low

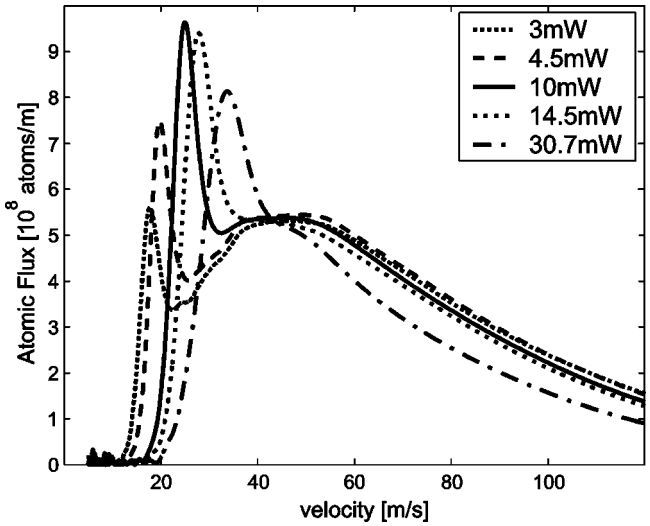

FIG. 9. When a laser beam is shone on the axis copropagating with the atomic beam, the longitudinal velocity distribution changes dramatically. A narrow peak arises at velocities between 20 m/s and 40 m/s. Its width and position on the v_z axis depend on the intensity in the pushing beam. Atoms at very low velocities below 15 m/s are pushed out of the beam or are accelerated. The total flux stays nearly constant.

velocities (centered around 25 m/s) arises. The width of this feature increases and its position is shifted toward higher values when the power in the pushing beam is increased. Since there is no magnetic field gradient on the axis, the axial beam addresses only a certain velocity class of atoms. The data indicate that a group of atoms propagating in the negative z direction is slowed down and their direction of propagation is turned around to the positive z direction. At the same time the very slow atoms are pushed out of the beam. The velocity distribution shows almost no atoms at velocities below 15 m/s. The total flux stays nearly constant when the pushing beam is shone in. Only for high powers (above 15 mW) in the pushing beam is the 2D MOT too much disturbed and the flux decreases as is shown by the curve for 30.7 mW in Fig. 9. A different detuning in the axial beams from the usual MOT laser beams could address the high velocity classes and increase the number of slow atoms in the beam. This slowing effect can be used to increase the flux at low velocities, which might be useful when loading conventional 3D MOT configurations with capture ranges around 30 m/s.

V. SUMMARY AND OUTLOOK

We realized and investigated a 2D MOT source of cold Rb atoms using four independent transverse laser beams for cooling. The underlying physics is pure two-dimensional cooling and trapping. To reach a high flux with a small divergence we work at high vapor pressures and high intensities of the laser fields, and use a differential pumping tube of large diameter that extracts most of the atoms cooled in the 2D MOT. This results in a different form of the velocity distribution compared to that in [21]. We observe a higher mean velocity of about 50 m/s and a higher total flux. The total flux is in the range of several 10^{10} atoms/s. A maximum flux of 6×10^{10} atoms/s was obtained at a 2D MOT length of 90 mm, laser intensity of 160 mW per beam, and vapor pressure in the glass cell of 1.6×10^{-6} mbar. If we integrate the brightness over the output area of our source we obtain 7.5×10^{13} atoms/s sr. Also, for low laser powers and a comparable configuration of the 2D MOT we observe a broad velocity distribution as shown in Fig. 3, which differs from that of [21]. The length of the 2D MOT provides good collimation resulting in a divergence of 32 mrad, which is not geometrically limited by the differential pumping tube.

This alternative source of atoms provides a total flux comparable to that of a Zeeman slower with less total length, less material throughput, and without disturbing light and magnetic fields for a consecutive MOT in a UHV system. It makes a fast and efficient trapping of a large number of atoms in a magneto-optical trap feasible and therefore provides a very good starting point for further laser and evaporative cooling experiments and Bose-Einstein Condensate generating apparatus [27,28].

In a consecutive experiment we loaded the atom beam into a 3D MOT with a capture velocity of about 50 m/s in a UHV environment of background pressure in the lower 10^{-11} mbar range. Using a laser power of 75 mW per beam we obtain a flux of 2×10^{10} atoms/s and load of about 6×10^{10} atoms within 5 s loading time. When the shutter between the low vacuum and the UHV chamber was closed, lifetimes of the magnetically trapped atoms of up to 90 s were observed.

Additionally we presented an analytical model for describing the longitudinal velocity distribution and the dependence of the total flux on geometry and pressure in the vapor cell. As discussed in Sec. IV our model is in good agreement with the experimental results. The theoretical model and its experimental verification will be helpful for the design of intense sources in future laser-cooling experiments.

ACKNOWLEDGMENTS

This work was supported by the Schwerpunktprogramm ''Wechselwirkung in ultrakalten Atom- und Molekülgasen'' (SPP 1116) of the Deutsche Forschungsgemeinschaft and by the European Research Training Network ''Cold Quantum Gases'' under Contract No. HPRN-CT-2000-00125.

[1] C.S. Adams, M. Sigel, and J. Mlynek, Phys. Rep. **240**, 143 (1994).
[2] H. J. Metcalf and P. van der Straten, *Laser Cooling and Trapping* (Springer, New York, 1999).
[3] W. Ketterle and N.J. van Druten, Adv. At., Mol., Opt. Phys. **37**, 181 (1996).
[4] R. Watts and C. Wieman, Opt. Lett. **11**, 291 (1986).
[5] W. Phillips and H.J. Metcalf, Phys. Rev. Lett. **48**, 596 (1982).
[6] A. Steane, P. Szriftgiser, P. Desbiolles, and J. Dalibard, Phys. Rev. Lett. **74**, 4972 (1995).
[7] T.B. Swanson, D. Asgeirsson, J.A. Behr, A. Gorelov, and D. Melconian, J. Opt. Soc. Am. B **15**, 2641 (1998).
[8] K.H. Kim, K.I. Lee, H.R. Noh, W. Jhe, N. Kwon, and M. Ohtsu, Phys. Rev. A **64**, 013402 (2001).
[9] C.J. Myatt, N.R. Newbury, R.W. Ghrist, S. Loutzenhiser, and C.E. Wieman, Opt. Lett. **21**, 290 (1996).
[10] K. Gibble, S. Chang, and R. Legere, Phys. Rev. Lett. **75**, 2666 (1995).
[11] Y. Fukuyama, H. Kanou, V.I. Balykin, and K. Shimizu, Appl. Phys. B: Lasers Opt. **70**, 561 (2000).
[12] Z.T. Lu, K.L. Corwin, M.J. Renn, M.H. Anderson, E.A. Cornell, and C.E. Wieman, Phys. Rev. Lett. **77**, 3331 (1996).
[13] R.S. Williamson III, P.A. Voytas, R.T. Newell, and T. Walker, Opt. Express **3**, 111 (1998).
[14] A. Camposeo, A. Piombini, F. Cervelli, F. Tantussi, F. Fuso, and E. Arimondo, Opt. Commun. **200**, 231 (2001).
[15] J. Nellessen, J. Werner, and W. Ertmer, Opt. Commun. **78**, 300 (1990).
[16] E. Riis, D.S. Weiss, K.A. Moler, and S. Chu, Phys. Rev. Lett. **64**, 1658 (1990).
[17] J. Yu, J. Djemaa, P. Nosbaum, and P. Pillet, Opt. Commun. **112**, 136 (1994).

[18] T.B. Swanson, N.J. Silva, S.K. Mayer, J.J. Maki, and D.H. McIntyre, J. Opt. Soc. Am. B **13**, 1833 (1996).
[19] J.G.C. Tempelaars, R.J.W. Stas, P.G.M. Sebel, H.C.W. Beijerinck, and E.J.D. Vredenbregt, Eur. Phys. J. D **18**, 113 (2002).
[20] P. Berthoud, A. Joyet, G. Dudle, N. Sagna, and P. Thomann, Europhys. Lett. **41**, 141 (1998).
[21] K. Dieckmann, R.J.C. Spreeuw, M. Weidemüller, and J.T.M. Walraven, Phys. Rev. A **58**, 3891 (1998).
[22] H. Chen and E. Riis, Appl. Phys. B: Lasers Opt. **70**, 665 (2000).
[23] C. Monroe, W. Swann, H. Robinson, and C. Wieman, Phys. Rev. Lett. **65**, 1571 (1990).
[24] A.M. Steane, M. Chowdhury, and C.J. Foot, J. Opt. Soc. Am. B **9**, 2142 (1992).
[25] E.J.D. Vredenbregt, K.A.H. van Leeuwen, and H.C.W. Beijerinck, Opt. Commun. **147**, 375 (1998).
[26] M. H. Hablanian, *High-Vacuum Technology* (Dekker, New York, 1990).
[27] W. Ketterle, D. S. Durfee, and D. M. Stamper-Kurn, in *Bose-Einstein Condensation in Atomic Gases*, Proceedings of the International School of Physics ''Enrico Fermi,'' Course CXL (IOS Press, Amsterdam, 1999), pp. 67–176.
[28] E. Mandonnet, A. Minguzzi, R. Dum, I. Carusotto, Y. Castin, and J. Dalibard, Eur. Phys. J. D **10**, 9 (2000).